# Electroweak Phase Transition in the MSSM: 4-Dimensional Lattice Simulations

F. Csikor[a], Z. Fodor[a], P. Hegedüs[a], A. Jakovác[b], S. D. Katz[a], A. Piróth[a]

[a] *Institute for Theoretical Physics, Eötvös University, H-1117, Pázmány P. 1A, Budapest, Hungary*
[b] *Department of Theoretical Physics, Technical University, Budapest, H-1521, Budapest, Hungary*

(October 23, 2018)

Recent lattice results have shown that there is no Standard Model (SM) electroweak phase transition (EWPT) for Higgs boson masses above $\approx 72$ GeV, which is below the present experimental limit. According to perturbation theory and 3-dimensional (3d) lattice simulations there could be an EWPT in the Minimal Supersymmetric Standard Model (MSSM) that is strong enough for baryogenesis up to $m_h \approx 105$ GeV. In this letter we present the results of our large scale 4-dimensional (4d) lattice simulations for the MSSM EWPT. We carried out infinite volume and continuum limits and found a transition whose strength agrees well with perturbation theory, allowing MSSM electroweak baryogenesis at least up to $m_h = 103 \pm 4$ GeV. We determined the properties of the bubble wall that are important for a successful baryogenesis.

The visible Universe is made up of matter. This statement is mainly based on observations of the cosmic diffuse $\gamma$-ray background, which would be larger than the present limits if boundaries between "worlds" and "antiworlds" existed [1]. The observed baryon asymmetry of the universe was eventually determined at the EWPT [2]. On the one hand this phase transition was the last instance when baryon asymmetry could have been generated, around $T \approx 100 - 200$ GeV. On the other hand at these temperatures any B+L asymmetry could have been washed out. The possibility of baryogenesis at the EWPT is particularly attractive, since the underlying physics can be—and has already largely been—tested in collider experiments.

The first detailed description of the EWPT in the SM was based on perturbative techniques [3], which resulted in $\mathcal{O}(100\%)$ corrections between different orders of the perturbative expansion for Higgs boson masses larger than about 60 GeV. The dimensionally reduced 3d effective model (e.g. [4]) was also studied perturbatively and gave similar conclusions. Large scale numerical simulations both on 4d and 3d lattices were needed to analyze the nature of the transition for realistic Higgs boson masses [5,6]. These results are in complete agreement, and predict [7,8] an end point for the first order EWPT at Higgs boson mass $72.0 \pm 1.4$ GeV [8], above which only a rapid cross-over can be seen. The present experimental lower limit of the SM Higgs boson mass is by several standard deviations larger than the end point value, thus any EWPT in the SM is excluded. This also means that the SM baryogenesis in the early Universe is ruled out.

In order to explain the observed baryon asymmetry, extended versions of the SM are necessary. Clearly, the most attractive possibility is the MSSM. According to perturbative predictions the EWPT could be much stronger in the MSSM than in the SM [9], in particular if the stop mass is smaller than the top mass [10].

At two-loop level stop-gluon graphs give a considerable strengthening of the EWPT (e.g. third and fourth paper of [9]). A reduced 3d version of the MSSM has recently been studied on the lattice [11] (including $SU(3) \times SU(2)$ gauge fields, the right-handed stop and the "light" combination of the Higgses). The results show that the EWPT can be strong enough, i.e. $v/T_c > 1$, up to $m_h \approx 105$ GeV and $m_{\tilde{t}} \approx 165$ GeV (where $m_h$ is the mass of the lightest neutral scalar and $m_{\tilde{t}}$ is that of the stop squark). The possibility of spontaneous CP violation for a successful baryogenesis is also addresed [12].

In this letter we study the EWPT in the MSSM on 4d lattices and carry out infinite volume and continuum limit extrapolations. Except for the U(1) sector and scalars with small Yukawa couplings, the whole bosonic sector of the MSSM is kept: SU(3) and SU(2) gauge bosons, two Higgs doublets, left-handed and right-handed stops and sbottoms. As it has been done in the SM case [8], fermions, owing to their heavy Matsubara modes, are included perturbatively in the final result. This work extends the 3d study [11] in two ways:

a) We use 4d lattices instead of 3d. Note, that due to very soft modes—close to the end point in the SM—much more CPU time is needed in 4d than in 3d. However, this difficulty does not appear in the MSSM because the phase transition is strong and the dominant correlation lengths are not that large in units of $T_c^{-1}$. Using unimproved lattice actions the leading corrections due to the finite lattice spacings are proportional to $a$ in 3d and only to $a^2$ in 4d. For $O(a)$ improvement in the 3d case cf. [13]. In 4d simulations we also have direct control over zero temperature renormalization effects.

b) We include both Higgs doublets, not only the light combination. According to standard baryogenesis scenarios (see e.g. [14]) the generated baryon number is directly proportional to the change of $\beta$ through the bubble wall: $\Delta\beta$. ($\tan\beta = v_2/v_1$, where $v_{1,2}$ are the expectation
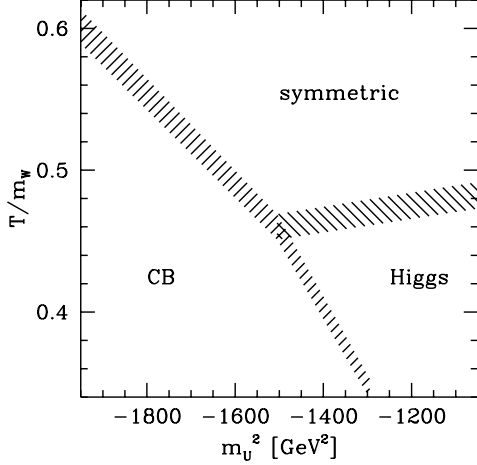
FIG. 1. The phase diagram of the bosonic theory obtained by lattice simulations.

values of the two Higgses.)

The continuum lagrangian of the above theory in standard notation reads

$$\mathcal{L} = \mathcal{L}_g + \mathcal{L}_k + \mathcal{L}_V + \mathcal{L}_{sm} + \mathcal{L}_Y + \mathcal{L}_w + \mathcal{L}_s. \quad (1)$$

The gauge part, $\mathcal{L}_g = 1/4 \cdot F_{\mu\nu}^{(w)} F^{(w)\mu\nu} + 1/4 \cdot F_{\mu\nu}^{(s)} F^{(s)\mu\nu}$ is the sum of weak and strong terms. The kinetic part is the sum of the covariant derivative terms of the two Higgs doublets $(H_1, H_2)$, the left-handed stop-sbottom doublet $(Q)$, and the right-handed stop, sbottom singlets $(U, D)$: $\mathcal{L}_k = (\mathcal{D}_\mu^{(w)} H_1)^\dagger (\mathcal{D}^{(w)\mu} H_1) + (\mathcal{D}_\mu^{(w)} H_2)^\dagger (\mathcal{D}^{(w)\mu} H_2) + (\mathcal{D}_\mu^{(ws)} Q)^\dagger (\mathcal{D}^{(ws)\mu} Q) + (\mathcal{D}_\mu^{(s)} U^*)^\dagger (\mathcal{D}^{(s)\mu} U^*) + (\mathcal{D}_\mu^{(s)} D^*)^\dagger (\mathcal{D}^{(s)\mu} D^*)$. The potential term for the Higgs fields reads $\mathcal{L}_V = m_{12}^2 [\alpha_1 |H_1|^2 + \alpha_2 |H_2|^2 - (H_1^\dagger \tilde{H}_2 + h.c.)] + g_w^2/8 \cdot (|H_1|^4 + |H_2|^4 - 2|H_1|^2|H_2|^2 + 4|H_1^\dagger H_2|^2)$, for which two dimensionless mass terms are defined, $\alpha_1 = m_1^2/m_{12}^2$ and $\alpha_2 = m_2^2/m_{12}^2$. One gets $\mathcal{L}_{sm} = m_Q^2 |Q|^2 + m_U^2 |U|^2 + m_D^2 |D|^2$ for the squark mass part, and $\mathcal{L}_Y = h_t^2 (|QU|^2 + |H_2|^2|U|^2 + |Q^\dagger \tilde{H}_2|^2)$ for the dominant Yukawa part. The quartic parts containing the squark fields read $\mathcal{L}_w = g_w^2/8 \cdot [2\{Q\}^4 - |Q|^4 + 4|H_1^\dagger Q|^2 + 4|H_2^\dagger Q|^2 - 2|H_1|^2|Q|^2 - 2|H_2|^2|Q|^2]$ and $\mathcal{L}_s = g_s^2/8 \cdot [3\{Q\}^4 - |Q|^4 + 2|U|^4 + 2|D|^4 - 6|QU|^2 - 6|QD|^2 + 6|U^\dagger D|^2 + 2|Q|^2|U|^2 + 2|Q|^2|D|^2 - 2|U|^2|D|^2]$, where $\{Q\}^4 = Q_{i\alpha}^* Q_{j\beta}^* Q_{i\beta} Q_{j\alpha}$. The scalar trilinear couplings have been omitted for simplicity. It is straightforward to obtain the lattice action, for which we used the standard Wilson plaquette, hopping and site terms.

The parameter space of the above Lagrangian is many-dimensional. We analyze the effect of the strong sector on the EWPT by using three specific sets of parameters. In one case the strong coupling has its physical value, whereas in the two other cases it is somewhat larger and smaller. The experimental values are taken for the weak and Yukawa couplings, and $\tan\beta = 6$ is

used. For the bare soft breaking masses our choice is $m_{Q,D} = 250$ GeV, $m_U = 0$ GeV. Lattice renormalization effects on these masses will be discussed later.

The simulation techniques are similar to those of the SU(2)-Higgs model [5] (overrelaxation and heatbath algorithms are used for each scalar and gauge field); some new methods will be published elsewhere [15]. The analysis is based on finite temperature simulations (in which the temporal extension of the lattice $L_t$ is much smaller than the spatial extensions $L_{x,y,z}$), and zero temperature ones (with $L_t \approx L_{x,y,z}$). For a given $L_t$, we fix all parameters of the Lagrangian except $\alpha_2$. We tune $\alpha_2$ to the transition point, $\alpha_{2c}$, where we determine the jump of the Higgs field, the shape of the bubble wall, and the change of $\beta$ through the phase boundary. Using $\alpha_{2c}$ and the parameter set of the finite temperature case, we perform $T = 0$ simulations and determine the masses (Higgses and W) and couplings (weak and strong) there. Extrapolations to the continuum limit and to infinite volumes are based on simulations at temporal extensions $L_t = 2, 3, 4, 5$ and at various lattice volumes for each $L_t$, respectively. Approaching the continuum limit, we move on an approximate line of constant physics (LCP), on which the renormalized quantities (masses and couplings) are almost constant, but the lattice spacing approaches zero. Our theory is bosonic, therefore the leading corrections due to finite lattice spacings are expected to be proportional to $a^2$. This lattice spacing dependence is assumed for physical quantities in $a \longrightarrow 0$ extrapolations.

We compare our simulation results with perturbation theory. We used one-loop perturbation theory without applying high temperature expansion (HTE). A specific feature was a careful treatment of finite renormalization effects, by taking into account all renormalization corrections and adjusting them to match the measured $T = 0$ spectrum [15]. We studied also the effect of the dominant $T \neq 0$ two-loop diagram ("setting-sun" stop-gluon graphs, cf. fifth ref. of [9]), but only in the HTE. We observed less dramatic enhancement of the strength of the phase transition due to two-loop effects than in [9]. Since the infrared behavior of the setting-sun graphs is not understood, we use the one-loop technique with the $T = 0$ scheme defined above. This type of one-loop perturbation theory is also applied to correct the measured data to some fixed LCP quantities, which are defined as the averages of results at different lattice spacings, (i.e. our reference point, for which the most important quantity is the lightest Higgs mass, $m_h \approx 45$ GeV).

Fig. 1. shows the phase diagram in the $m_U^2$–T plane. One identifies three phases. The phase on the left (large negative $m_U^2$ and small stop mass) is the "color-breaking" (CB) phase. The phase in the upper right part is the "symmetric" phase, whereas the "Higgs" phase can be found in the lower right part. The line separating the symmetric and Higgs phases is obtained from $L_t = 3$ simulations, whereas the lines between these phases and
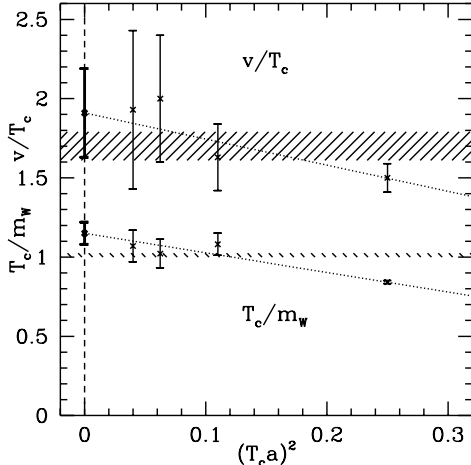
2

FIG. 2. The normalized jump and the critical temperature in the continuum limit.



FIG. 3. The cosmologically relevant $v/T_c > 1$ region is below the lines.

the CB one are determined by keeping the lattice spacing fixed while increasing and decreasing the temperature by changing $L_t$ to 2 and 4, respectively. The shaded regions indicate the uncertainty in the critical temperatures. The phase transition to the CB phase is observed to be much stronger than that between the symmetric and Higgs phases. The qualitative features of this picture are in complete agreement with perturbative and 3d lattice results [9–11]; however, our choice of parameters does not correspond to a two-stage symmetric-Higgs phase transition. In this two-stage scenario there is a phase transition from the symmetric to the CB phase at some $T_1$ and another phase transition occurs at $T_2 < T_1$ from the CB to the Higgs phase. It has been argued [16] that in the early universe no two-stage phase transition took place, therefore we do not study this possibility and the features of the CB phase any further.

The bare squark mass parameters $m_Q^2, m_U^2, m_D^2$ receive quadratic renormalization corrections. As it is well known, one-loop lattice perturbation theory is not sufficient to reliably determine these corrections, thus we use the following method. We first determine the position of the non-perturbative CB phase transitions in the bare quantities (e.g. the triple point or the T=0 transition for $m_U^2$ in Fig. 1). These quantities are compared with the prediction of the continuum perturbation theory, which gives the renormalized mass parameters on the lattice.

Fig. 2 contains the continuum limit extrapolation for the normalized jump of the order parameter ($v/T_c$: upper data) and the critical temperature ($T_c/m_W$: lower data). The shaded regions are the perturbative predictions at our reference point (see above) in the continuum. Their widths reflect the uncertainty of our reference point, which is dominated by the error of $m_h$. Note that $v/T_c$ is very sensitive to $m_h$, which results in the large uncertainties. Results obtained on the lattice and in perturbation theory agree reasonably within the esti-
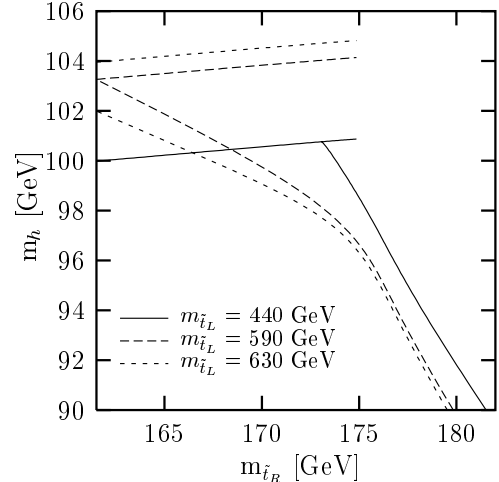
mated uncertainties. (It might well be that the $L_t=2$ results are not in the scaling region; leaving them out from the continuum extrapolation the agreement between the lattice and perturbative results is even better.)

Based on this agreement we use one-loop perturbation theory without HTE to determine cosmologically allowed regions in the $m_{\tilde{t}_R}$ vs. $m_h$ plane of the full MSSM (including fermions, $m_A = 500$ GeV), see Fig. 3. The two lines for each $m_{\tilde{t}_L}$ (which intersect for lower values of $m_{\tilde{t}_L}$) correspond to upper bounds resulting from $v_n/T_c = 1$ (steeper curves, B1) and the T=0 maximum MSSM Higgs mass (B2). $v_n$ is the non-perturbative Higgs expectation value, assumed to be larger than the perturbative one by 14%, a correction factor obtained in the bosonic model (cf. Fig. 2). For large $m_Q$ (e.g. 600 GeV, $m_{\tilde{t}_L}=630$ GeV) the region below B1 is below B2. Decreasing $m_Q$ B2 decreases and B1 increases. At $m_Q=560$ GeV ($m_{\tilde{t}_L}=590$ GeV) B1 and B2 intersect at the CB value of $m_{\tilde{t}_R}$. Since B2 is almost constant this yields the overall maximum Higgs mass for a successful baryogenesis. For even smaller $m_Q$ ($m_{\tilde{t}_L}$) both B1 and B2 are relevant. Note that the maximum Higgs mass corresponds to a finite value of $m_Q \approx 560$ GeV, yielding $m_h = 103 \pm 4$ GeV (including also the uncertainties from Fig. 2 and the difference between the one and two-loop maximum Higgs mass calculations [17]).

In order to produce the observed baryon asymmetry, a strong first order phase transition is not enough. According to standard MSSM baryogenesis scenarios [14] the generated baryon asymmetry is directly proportional to the variation of $\beta$ through the bubble wall separating the Higgs and symmetric phases. By using elongated lattice $(2 \cdot L^2 \cdot 192)$, L=8,12,16 at the transition point we study the properties of the wall. In our simulation procedure we restrict the length of one of the Higgs fields to a small interval between its values in the bulk phases. As a consequence, the system fluctuates around a con-
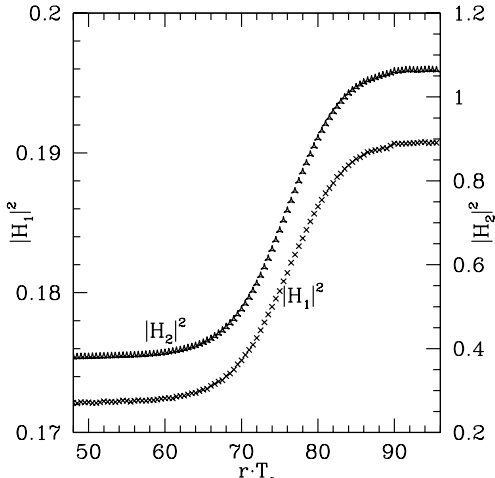
FIG. 4. The profile of the bubble wall for both of the Higgs fields for the lattice $2 \cdot L^2 \cdot 192$.

figuration with two bulk phases and two walls between them. In order to have the smallest possible free energy, the wall is perpendicular to the long direction. We eliminate the effect of the remaining zero mode by shifting the wall of each configuration to some fixed position. Fig.4 gives the bubble wall profiles for both Higgs fields. The measured width of the wall is $[A + B \cdot \log(aLT_c)]/T_c$ $A = 10.8 \pm .1$ and $B = 2.1 \pm .1$. This behavior indicates that the bubble wall is rough and without a pinning force of finite size its width diverges very slowly (logarithmically) [18]. For the same bosonic theory the perturbative approach predicts $(11.2 \pm 1.5)/T_c$ for the width.

Transforming the data of Fig. 4 to $|H_2|^2$ as a function of $|H_1|^2$, we obtain $\Delta\beta = 0.0061 \pm 0.0003$. The perturbative prediction at this point is $0.0046 \pm 0.0010$. Thus perturbative studies such as [19] are confirmed by non-perturbative results.

To summarize, we presented 4d lattice results on the EWPT in the MSSM. Our simulations were carried out in the bosonic sector of the MSSM. We found quite a good agreement between lattice results and our one-loop perturbative predictions. Using this agreement together with a careful analysis of its uncertainties, we determined the upper bound for the lightest Higgs mass for a successful baryogenesis in the full (bosonic+fermionic) MSSM, which turned out to be $(103 \pm 4 \text{ GeV})$ consistent with the 3d analysis ($\approx 105$ GeV). We analyzed the bubble wall profile separating the Higgs and symmetric phases. The width of the wall and the change in $\beta$ is in fairly good agreement with perturbative predictions for typical bubble sizes. Both the upper bound for $m_h$ and the smallness of $\Delta\beta$ indicate that experiments allow just a small window for MSSM baryogenesis.

Details of the present analysis will be discussed in a forthcoming publication [15].

[1] A. G. Cohen, A. De Rujula, S. L. Glashow, Astrophys. J. **495** (1998) 539.
[2] V. A. Kuzmin, V. A. Rubakov and M. E. Shaposhnikov, Phys. Lett. **B155** (1985) 36.
[3] P. Arnold and O. Espinosa, Phys. Rev. **D47**, 3546 (1993), erratum ibid., **D50**, 6662 (1994); W. Buchmüller et al., Ann. Phys. (NY) **234**, 260 (1994); Z. Fodor and A. Hebecker, Nucl. Phys. **B432**, 127 (1994).
[4] K. Farakos et al., Nucl. Phys. **B425**, 67 (1994); A. Jakovác and A. Patkós, Nucl. Phys. **B494**, 54 (1997).
[5] B. Bunk et al., Nucl. Phys. **B403**, 453 (1993), Z. Fodor et al., Phys. Lett. **B334**, 405 (1994); Nucl. Phys. **B439**, 147 (1995), F. Csikor et al., Nucl. Phys. **B474**, 421 (1996).
[6] K. Kajantie et al., Nucl. Phys. **B407**, 356 (1993); Nucl. Phys. **B466**, 189 (1996); O. Philipsen et al., Nucl. Phys. **B469**, 445 (1996).
[7] K. Kajantie et al., Phys. Rev. Lett. **77**, 2887 (1996); F. Karsch et al., Nucl. Phys. B (Proc. Suppl.) **53**, 623 (1997); M. Gürtler et al., Phys. Rev. **D56**, 3888 (1997).
[8] F. Csikor et al., Phys. Rev. Lett. **82**, 21 (1999) (for analytical end point results see second paper of [3] and W. Buchmüller, O. Philipsen, Nucl. Phys. **B443** 47 (1995)).
[9] G. F. Guidice, Phys. Rev. **D45**, 3177 (1992); J. R. Espinosa et al., Phys. Lett. **B307**, 106 (1993); A. Brignole et al., Phys. Lett. **B324**, 181 (1994); J. R. Espinosa, Nucl. Phys. **B475**, 273 (1996); B. de Carlos, J. R. Espinosa, Nucl. Phys. **B503**, 24 (1997); D. Bödeker et al., Nucl. Phys. **B497**, 387 (1997); J. M. Cline, G. D. Moore, Phys. Rev. Lett. **81**, 3315 (1998) M. Losada, Nucl. Phys. **B537**, 3 (1999); hep-ph/9905441.
[10] M. Carena et al., Phys. Lett. **B380**, 81 (1996); Nucl. Phys. **B524** 3 (1998).
[11] M. Laine, K. Rummukainen, Phys. Rev. Lett. **80** 5259 (1998); Nucl. Phys. **B535** 423 (1998).
[12] K. Funakubo et al., Prog. Theor. Phys. **99** 1045 (1998); ibid., **102** 389 (1999); M. Laine, K. Rummukainen, Nucl. Phys. **B545** 141 (1999); hep-lat/9908045.
[13] G. D. Moore, Nucl. Phys. **B523**, 569 (1998).
[14] P. Huet, A. E. Nelson, Phys. Rev. **D53**, 4578 (1996); Phys. Lett. **B355**, 229 (1995); M. Carena et al., Nucl. Phys. **B503**, 387 (1997); A. Riotto, Nucl. Phys. **B518**, 339 (1998); Phys. Rev. **D58** 095009 (1998); N. Rius, V. Sanz, hep-ph/9907460; M. Brhlik, et al., hep-ph/9911243.
[15] F. Csikor, Z. Fodor, P. Hegedüs, A. Jakovác, S. D. Katz, A. Piróth, in preparation.
[16] J. M. Cline et al., Phys. Rev. **D60**, 105035 (1999).
[17] M. Carena et al., hep-ph/0001002.
[18] D. Jasnow, Rep. Prog. Phys. **47**, 1059 (1984)
[19] J. M. Moreno et al., Nucl. Phys. **B526**, 489 (1998); P. John, Phys. Lett. **B452**, 221 (1999).